Hesperetin induces apoptosis in lung squamous carcinoma cells via G_2/M cycle arrest, inhibition of the Notch1 pathway and activation of endoplasmic reticulum stress

QIANLONG XIE[1,2], ZIMING HE[2], LINGFANG TAN[2], MIN LI[3], MIN ZHUANG[2], CHEN LIU[4], SUNHUI CHEN[5,6], LONG JIN[7,8] and YUXIA SUI[5,6]

[1]Department of Pharmacy, Wuping County Hospital, Longyan, Fujian 363400, P.R. China; [2]School of Pharmacy, Fujian Medical University, Fuzhou, Fujian 350122, China; [3]Department of Clinical Laboratory, Fuzhou University Affiliated Provincial Hospital, Fuzhou, Fujian 350001, P.R. China; [4]School of Basic Medical Sciences, Fujian Medical University, Fuzhou, Fujian 350122, P.R. China; [5]Department of Pharmacy, Fuzhou University Affiliated Provincial Hospital, Fuzhou, Fujian 350001, P.R. China; [6]Department of Pharmacy, Shengli Clinical Medical College of Fujian Medical University, Fuzhou, Fujian 350001, P.R. China; [7]Department of Pathology, Fuzhou University Affiliated Provincial Hospital, Fuzhou, Fujian 350001, P.R. China; [8]Department of Pathology, Shengli Clinical Medical College of Fujian Medical University, Fuzhou, Fujian 350001, P.R. China

Received October 22, 2024; Accepted February 20, 2025

DOI: 10.3892/ijmm.2025.5518

Abstract. Hesperetin (HST), a natural flavonoid, has potent antitumor effects on lung adenocarcinoma; however, its effects on lung squamous cell carcinoma (LUSC) are currently unknown. The present study aimed to investigate the anticancer effects of HST on LUSC cells. The influence of 37.5, 75 and 150 μM HST on the H1703 cell line, and of 75, 150 and 300 μM HST on the H226 cell line was determined using the Cell Counting Kit-8 method, cell cycle assay, JC-1 mitochondrial membrane potential assay and Annexin V-FITC/PI staining. DMSO-treated cells were used as the control group. Western blotting was performed to detect the protein expression levels of cyclin B1, CDK1, Bcl-2, Bax, caspase-3, cleaved caspase-3, phosphorylated-eIF2α, eIF2α, glucose-regulated protein 78, CHOP, Notch1 and Hes-1. The relationship between endoplasmic reticulum stress (ERS), Notch1 signaling and apoptosis was examined using the ERS-inhibitor 4-phenylbutyric acid (4-PBA; 500 μM) and the Notch1 signaling activator Jagged-1 (4 μM). *In vivo*, mice were divided into control, HST (30, 60 and 90 mg/kg/q2d) and cisplatin (2 mg/kg/q2d) groups to evaluate the anti-LUSC effects of HST. The results revealed that HST inhibited the viability of H226 and H1703 cells, leading to cell cycle arrest at the G_2/M phase and the induction of cell apoptosis. In addition, HST downregulated the Notch1 signaling pathway and increased ERS. In H1703 cells, 4-PBA and Jagged-1 reduced the expression of apoptosis-related proteins, and Jagged-1 also reduced the expression of ERS-related proteins. *In vivo*, HST reduced tumor growth without any apparent toxic side effects. In conclusion, HST may exert its antitumor effects by inducing G_2/M cell cycle arrest and inhibiting the Notch1 signaling pathway to activate ERS-induced apoptosis, making it a promising agent for treating LUSC.

Correspondence to: Mr. Long Jin, Department of Pathology, Fuzhou University Affiliated Provincial Hospital, 134 Dong Street, Fuzhou, Fujian 350001, P.R. China
E-mail: jinlongdoctor@163.com

Dr Yuxia Sui, Department of Pharmacy, Fuzhou University Affiliated Provincial Hospital, 134 Dong Street, Fuzhou, Fujian 350001, P.R. China
E-mail: syxfj123@163.com

Key words: lung squamous cell carcinoma, hesperetin, apoptosis, G_2/M phase arrest, Notch1 pathway, endoplasmic reticulum stress

Introduction

Lung cancer is a malignant tumor that has high morbidity and mortality rates worldwide; this type of cancer can be divided into small-cell lung cancer (SCLC) and non-SCLC (NSCLC). Worldwide, NSCLC accounts for 80-85% of all lung cancer cases and the 5-year survival rate is generally <30% (1). Lung squamous cell carcinoma (LUSC) accounts for ~30% of all NSCLC cases worldwide. Owing to the low mutation rate in its driver genes, there is a lack of effective targeted drugs for LUSC (2), and patients with advanced LUSC are treated primarily with chemotherapy, which has significant toxic side effects (e.g., Bone marrow suppression and neurotoxicity) and is associated with a poor prognosis (3). Therefore, there is an urgent clinical need for the identification of effective treatments for LUSC with minimal side effects.

In recent years, the potential role and advantages of flavonoids in lung cancer treatment have attracted considerable interest. These compounds exhibit antitumor effects through multiple mechanisms, including cell cycle regulation, apoptosis induction and inhibition of tumor angiogenesis. Their

wide availability, low toxicity and capacity to synergize with other therapeutic modalities confer favorable biocompatibility and significant antitumor efficacy, while minimizing damage to normal cells (4). Hesperetin (HST) is a natural flavonoid in citrus, grapefruit and other fruits, which has diverse pharmacological effects, including anti-inflammatory, antioxidant, antiviral and antihypertensive activities (5). Notably, the antitumor effects of HST have garnered attention, and studies have shown that HST has inhibitory effects on various types of cancer, such as lung adenocarcinoma, and stomach, esophageal, breast, colon, prostate and thyroid cancer (6-10). To the best of our knowledge, there are no studies on HST in LUSC.

To address the urgent clinical need for effective and low-toxicity treatments for LUSC, the present study is the first, to the best of our knowledge, to report on the *in vitro* and *in vivo* anti-LUSC effects of HST. The current study investigated the molecular mechanisms of HST-induced apoptosis in LUSC cells by assessing apoptosis-related signaling, focusing on the endoplasmic reticulum stress (ERS) and Norch1 signaling pathways as potential targets.

As precision medicine continues to advance, therapeutic strategies for LUSC are also being refined. Future research directions are likely to encompass the development of novel biomarkers to facilitate personalized treatments. The current study not only offers novel insights into the treatment of LUSC but also establishes a foundation for the further exploration of the clinical potential of HST.

Materials and methods

Cell lines and reagents. Human lung squamous carcinoma cell lines H226 (CRL-5826) and H1703 (CRL-5889) were obtained from the American Type Culture Collection. H226 and H1703 cells were cultured in RPMI 1640 (cat. no. PM150110; Wuhan Pricella Biotechnology Co., Ltd.) containing 10% fetal bovine serum (cat. no. A5669701; Gibco; Thermo Fisher Scientific, Inc.) and 1% penicillin-streptomycin solution (cat. no. MA0110; Dalian Meilun Biology Technology Co., Ltd.) at 37˚C in a 5% CO_2-humidified incubator.

Cell Counting Kit (CCK)-8 was purchased from APeXBIO Technology LLC (cat. no. K1018). The Cell Cycle and Apoptosis Analysis Kit (cat. no. C1052) and the mitochondrial membrane potential assay kit with JC-1 (cat. no. C2006) were obtained from Beyotime Institute of Biotechnology. The Annexin V-FITC Apoptosis Detection Kit was obtained from BD Biosciences (cat. no. 556547). Trypsin/ethylenediaminetetraacetic acid was purchased from Dalian Meilun Biology Technology Co., Ltd. (cat. no. MA0233). Primary antibodies against cyclin B1 (1:1,000; cat. no. 12231), phosphorylated (P-)eIF2α (Ser51) (1:1,000; cat. no. 9721), eIF2α (1:1,000;cat. no. 5324), CHOP (1:1,000; cat. no. 2895), Bax (1:1,000;cat. no. 5023) and cleaved caspase-3 (1:1,000; cat. no. 9661), and HRP-conjugated secondary antibodies (1:1,000; goat anti-rabbit IgG: cat. no. 7074; goat anti-mouse IgG cat. no. 7076) were obtained from Cell Signaling Technology, Inc. Primary antibodies against Notch1 (-1:1,000; cat. no. ab52627), Hes1 (1:1,000 cat. no. ab108937), caspase-3 (1:1,000; cat. no. ab32351), Bcl-2 (1:1,000; cat. no. ab182858), CDK1 (1:1,000; cat. no. ab133327) and glucose-regulated protein 78 (Grp78; 1:1,000; cat. no. ab108615) were obtained from Abcam. The GAPDH antibody (1:5,000; cat. no. 60004-1-Ig) was obtained from Proteintech Group, Inc.

HST (cat. no. HY-N0168), cisplatin (cat. no. HY-17394), 4-phenylbutyric acid (4-PBA; cat. no. HY-A0281), Jagged-1 (cat. no. HY-P1846A) and Ultra High Sensitivity ECL Kit (cat. no. HY-K1005) were purchased from MedChemExpress. HST was dissolved in DMSO to 400 mM and diluted with the culture medium to the desired concentration (the final DMSO concentration in the culture medium was <0.1%).

CCK-8 assay. To determine cell viability, the H226 and H1703 cells were adjusted to $4.0x10^4$ cells/ml and were inoculated into 96-well plates. The plates were incubated overnight in a cell culture incubator at 37˚C and 5% CO_2. The experimental groups were treated with HST at concentrations of 18.75, 37.5, 75, 150 300, 600 and 1,200 μM, whereas the control group was untreated. Incubation was performed at 37˚C for 24, 48 and 72 h. Each group comprised five composite wells. At 24, 48 and 72 h, the medium was removed, serum-free medium containing 10% CCK-8 was added, and the cells were incubated at 37˚C for 1-2 h. A microplate reader (SpectraMax iD5; Molecular Devices, LLC) was used to measure absorbance (OD) at a wavelength of 450 nm to calculate the cell survival rate in each well. The cell survival rate was calculated as follows: Cell survival rate (%)=$[(OD_{\text{experimental well}}-OD_{\text{blank well}})/(OD_{\text{control well}}-OD_{\text{blank well}})]$ x100.

Cell treatment. Based on the results of the CCK-8 assay, the experimental group was treated with HST at concentrations of 75, 150 and 300 μM for H226 cells, and 37.5, 75 and 150 μM for H1703 cells, whereas the control group was untreated. Incubation was performed at 37˚C for 48 h.

Cell cycle detection. Following HST treatment, the H226 and H1703 cells were collected, adjusted to $3x10^5$ cells/ml and precipitated by centrifugation at 1,000 x g for 5 min at 4˚C. Subsequently, 1 ml precooled 70% ethanol was added and the cells were fixed overnight at 4˚C. The cells were then centrifuged at 1,000 x g for 5 min at 4˚C and suspended in 0.5 ml PI staining solution containing RNase before being incubated at 37˚C for 30 min. Within 1 h, the cells were detected using flow cytometry (BD Accuri C6 Plus; Becton, Dickinson and Company) and cell cycle progression was analyzed using ModFit LT 5.0 software (Verity Software House, Inc.).

Analysis of mitochondrial membrane potential. Carbonyl cyanide m-chlorophenylhydrazone (CCCP) functions as a mitochondrial uncoupler and induces apoptosis through the dissipation of the mitochondrial membrane potential (11). The positive control group was treated with 50 μM CCCP for 30 min at 37˚C (data not shown). Following treatment, the H226 and H1703 cell density was adjusted to $5x10^5$ cells/ml, and the JC-1 staining working solution (0.5 ml) was added and mixed according to the manufacturer's instructions. After incubation at 37˚C in the dark for 20 min, the cells were washed, collected in JC-1 staining buffer (1X) and examined using a flow cytometer (BD Accuri C6 Plus) within 30 min. The results were analyzed using FlowJo 10.8.1 software (BD Biosciences).

Apoptosis assay. To quantify the rate of apoptosis, flow cytometry was performed according to the instructions of the Annexin V-FITC apoptosis detection kit. After treatment, the H226 and H1703 cells were harvested promptly by trypsinization, then resuspended in culture medium. The cells were then collected and adjusted to a concentration of $3x10^6$ cells/ml. Annexin V-FITC/PI staining was performed according to the manufacturer's protocol; the cell suspension and dye were thoroughly mixed, followed by incubation in the dark at 25˚C for 15 min. Detection was carried out within 1 h using a flow cytometer (BD Accuri C6 Plus). The results were analyzed using the accompanying CSampler Plus software v 1.0.34.1 (Becton, Dickinson and Company).

Xenograft model. Animal experiments were reviewed and approved by the Experimental Animal Welfare Ethics Committee of Fujian Provincial Hospital [approval no. IACUC-FPH-PZ-20240424(0006); Fuzhou, China]. Notably, Fujian Provincial Hospital was renamed to Fuzhou University Affiliated Provincial Hospital in 2024. Female BALB/c nude mice were purchased from Shanghai Lesk Experimental Animal Co. (cat. no. SDK111083). A total of 30 nude mice (age, 3-5 weeks; weight, 15-16 g), were housed in a specific pathogen-free barrier environment throughout the study. The ambient temperature was maintained at 20-25˚C, and the relative humidity was kept at 40-60%. The animals were fed sterilized specialized feed, with *ad libitum* access to food and water, and were maintained under a 12-h light/dark cycle. To establish a xenograft tumor model, $1x10^6$ H226 cells (100 μl) were injected subcutaneously into mice. The tumor volume was calculated, and when it reached 80-100 mm^3, the nude mice were divided into five groups: Mice in the control group were intraperitoneally injected with 0.2 ml 0.9% normal saline once every 2 days; mice in the treatment groups were intraperitoneally injected with 30, 60 or 90 mg/kg HST once every 2 days; and mice in the positive control group were administered cisplatin (2 mg/kg) intraperitoneally every 2 days. After 28 days of intervention, the mice were sacrificed. For euthanasia, mice were exposed to 60% vol/min CO_2 and subsequently underwent cervical dislocation. Transplanted tumors and major organs, such as the heart, liver and kidneys, were subsequently isolated, and inhibition rate of tumor weight was calculated as follows: Tumor inhibition rate (%)=(mean tumor weight of the control group-mean tumor weight of the intervention group)/mean tumor weight of the control group x100. The following humane endpoints were adhered to: i) Inability to move or lack of response to gentle stimulation; ii) difficulty breathing; iii) diarrhea or urinary incontinence; iv) weight loss of 20% of body weight before the experiment; v) inability to eat or drink; vi) obvious anxiety, irritability or tumor weight exceeds 10% of body weight; vii) skin damage occurred on >30% of body surface area, or infection and suppuration occur.

The transplanted tumors, heart, liver and kidney were fixed in 4% paraformaldehyde solution at room temperature for 24 h, then embedded in paraffin and sectioned into 5-μm slices. The sections were dewaxed and stained with hematoxylin for 5 min and eosin for 4 min at room temperature. Images of the stained sections were captured using a light microscope (Leica DM2000 LED; Leica Microsystems, Inc.). The protein expression levels in the transplanted tumors were detected by western blotting. A schematic diagram illustrating the animal experimentation process is presented in Fig. 1.

Western blot analysis. The treated lung cancer cell lines H226 and H1703, as well as xenograft tumor tissues derived from H226 cells in nude mice, were utilized for western blot analysis. Total protein was extracted using lysis buffer (cat. no. R0010; Beijing Solarbio Science & Technology Co., Ltd.) containing phenylmethanesulfonyl fluoride (cat. no. P0100; Beijing Solarbio Science & Technology Co., Ltd.) on ice for 5 min. Protein concentration was determined using a BCA protein assay kit (cat. no. ZJ102; Epizyme; Ipsen Pharma). The protein samples (30 μg) were then separated by sodium dodecyl sulfate-polyacrylamide gel electrophoresis (resolving gel concentrations, 6, 10 and 12.5%; 5% stacking gel), followed by transfer onto PVDF membranes (cat. no. ISEQ00005; MilliporeSigma). After blocking them with 5% skimmed milk powder in TBS-Tween (0.1%) at room temperature for 1 h, the membranes were incubated with specific primary antibodies overnight at 4˚C. After washing, the membranes were incubated with the corresponding secondary antibodies at room temperature for 1 h. The blots were visualized using the Ultra High Sensitivity ECL Kit (cat. no. HY-K1005; MedChemExpress) according to the manufacturer's instructions. The target band levels were analyzed and semi-quantified using ImageJ image analysis software (version 1.54k; National Institutes of Health).

Statistical analysis. All quantitative tests were repeated at least three times and the results are presented as the mean ± SEM. GraphPad Prism software (version 9.0; Dotmatics) was used for statistical analyses and image drawing. Comparisons between two groups were assessed using unpaired Student's t-test and differences between >2 groups were analyzed using a one-way ANOVA followed by Tukey's multiple comparisons post hoc test. For non-parametric data, the Mann-Whitney U test was used to compare two groups, whereas the Kruskal-Wallis test and Dunn's post hoc test was used to compared >2 groups. A two-way ANOVA followed by Tukey's multiple comparisons post hoc test was performed to evaluate the interactive effects of treatment duration and concentration. $P<0.05$ was considered to indicate a statistically significant difference.

Results

HST reduces the viability of H226 and H1703 cells. HST inhibited the viability of LUSC in a concentration- and time-dependent manner (Table I). Compared with in the control group, the survival rate of H226 cells after 48 h of treatment with 300 μM HST was 49.74±0.59%. The survival rate of H1703 cells was 65.28±0.71% after treatment with 150 μM HST for 48 h. These specific concentrations and durations were considered as optimal for eliciting significant cytotoxic effects while maintaining experimental feasibility. Notably, H1703 cells were more sensitive to HST than H226 cells. To avoid an excessive amount of cell death that would affect the accuracy and reproducibility of the experiment, subsequent experiments were performed following treatment with HST for 48 h; with 0, 75, 150 and 300 μM concentrations used to treat H226 cells and 37.5, 75 and 150 μM for H1703 cells.

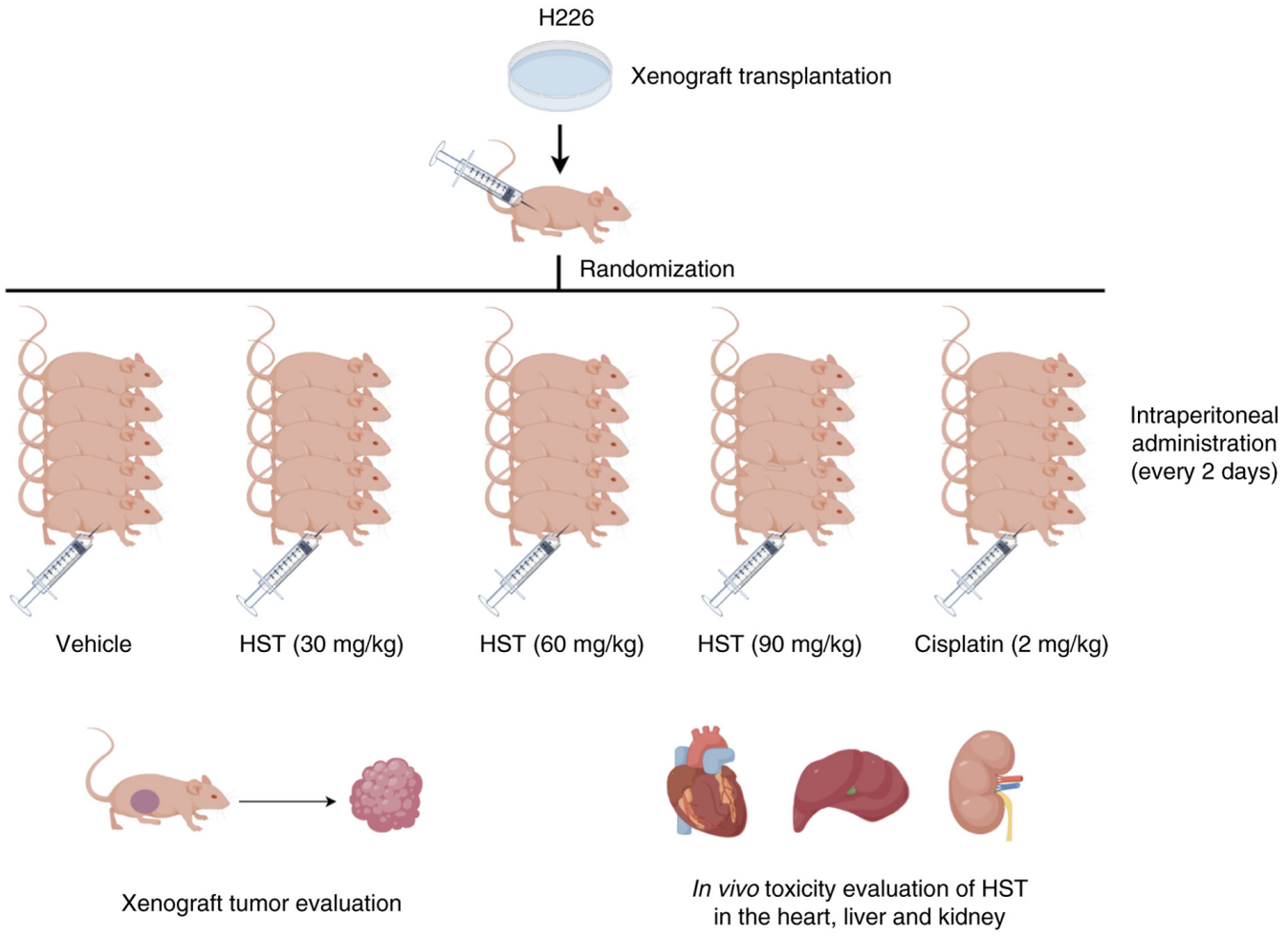

Figure 1. A schematic diagram of the animal experimentation process, which was drawn using Figdraw (https://www.figdraw.com/). HST, hesperetin.

HST induces a G_2/M phase cell cycle block in H226 and H1703 cells. After 48 h of treatment of H226 cells with different concentrations of HST, there was a significant increase in the proportion of cells in the G_2/M phase (Fig. 2A). Specifically, in the 75, 150 and 300 μM groups, the respective increases were 1.85±0.13, 5.88±0.15 and 12.13±0.24% compared with that in the control group. Conversely, the proportion of G_0/G_1 phase cells in the 150 and 300 μM groups was decreased by 2.72±0.12 and 23.02±3.16%, respectively. Notably, no significant pattern was observed in the number of S-phase cells. Similarly, when H1703 cells were treated with 37.5, 75 and 150 μM HST, the proportion of cells in G_2/M phase were increased by 0.67±0.50, 6.89±0.10 and 9.33±0.27%, respectively. Accordingly, the proportion of cell in the G_0/G_1 phase was decreased by 0.02±0.25, 14.26±1.43 and 11.17±0.69%, respectively. Notably, no significant trend was observed regarding the number of S-phase cells. Consequently, HST effectively blocked the LUSC cell cycle in the G_2/M phase and suppressed the proliferative capacity of cells.

To further investigate the mechanism underlying the effects of HST on cell cycle blockade in H226 and H1703 cells, the current study examined the expression levels of two proteins (Cyclin B1 and CDK1) that regulate the G_2/M phase. Compared with those in the control group, the expression levels of cyclin B1 in H226 cells were not significantly decreased in the 75 and 150 μM HST groups, whereas the levels of CDK1 were significantly reduced in the 150 μM group, and the protein expression levels of cyclin B1 and CDK1 were significantly decreased in the 300 μM group (Fig. 2B). Similarly, 75 μM HST decreased cyclin B1 and CDK1 protein expression levels in H1703 cells, but this was not statistically significant. However, treatment with 150 μM HST significantly reduced the protein expression levels of cyclin B1 and CDK1

HST induces apoptosis in H226 and H1703 cells. To determine whether the anti-proliferative effects of HST on H226 and H1703 cells were related to apoptosis, cell apoptosis was examined using PI and Annexin V-FITC double staining, and flow cytometry. The rate of apoptosis gradually increased with increasing HST concentrations (Fig. 3A). After 48 h of treatment with different concentrations of HST, the apoptosis rate of H226 cells increased from 11.03±1.32 to 28.63±1.01%. In addition, the apoptosis rate of H1703 cells increased from 7.33±0.52 to 49.73±1.50%, which was statistically significant compared with in the control group. These findings indicated that HST may induce the apoptosis of LUSC cells in a concentration-dependent manner.

Decreased mitochondrial membrane potential levels are early markers of apoptosis. The JC-1 polymer/monomer

Table I. Effect of HST on the survival rate of H226 and H1703 cells.

	H226			H1703		
HST, μM	24 h	48 h	72 h	24 h	48 h	72 h
0	100±1.702	100±0.64	100±1.07	100±2.18	100±0.39	100±2.25
18.75	98.36±1.13	95.42±0.31	98.63±3.41	93.41±0.93	91.74±0.76	93.62±0.58
37.5	94.46±0.93	95.32±0.98	96.99±0.73	91.54±0.27	86.36±1.59	85.51±0.78^{d}
75	95.38±1.50	94.79±1.77	95.44±0.93^{a}	89.39±0.59	79.379±1.35^{a,d}	72.48±0.36^{a,e}
150	86.05±1.51^{b}	79.00±0.06^{c,e}	75.33±0.56^{a,e}	83.60±1.03	65.28±0.71^{c,e}	48.31±0.89^{c,e}
300	71.69±0.14^{a}	49.74±0.59^{b,e}	36.64±0.50^{b,e}	66.39±1.72^{b}	37.26±0.23^{b,f}	23.25±0.65^{c,e}
600	40.56±0.21^{c}	22.55±0.53^{b,e}	3.24±0.27^{b,e}	40.47±0.79^{c}	9.25±0.07^{b,e}	1.47±0.24^{c,e}
1200	1.89±0.20^{b}	0.56±0.27^{b}	0.01±0.03^{b}	0.85±0.08^{b}	0.61±0.24^{b}	0.11±0.05^{b,f}

Data are presented as the mean ± SEM (n=5). ^{a}P<0.05, ^{b}P<0.001, ^{c}P<0.01 vs. control group at the same intervention time; ^{d}P<0.05, ^{e}P<0.001, ^{f}P<0.01 vs. 24-h group at the same intervention concentration. HST, hesperetin.

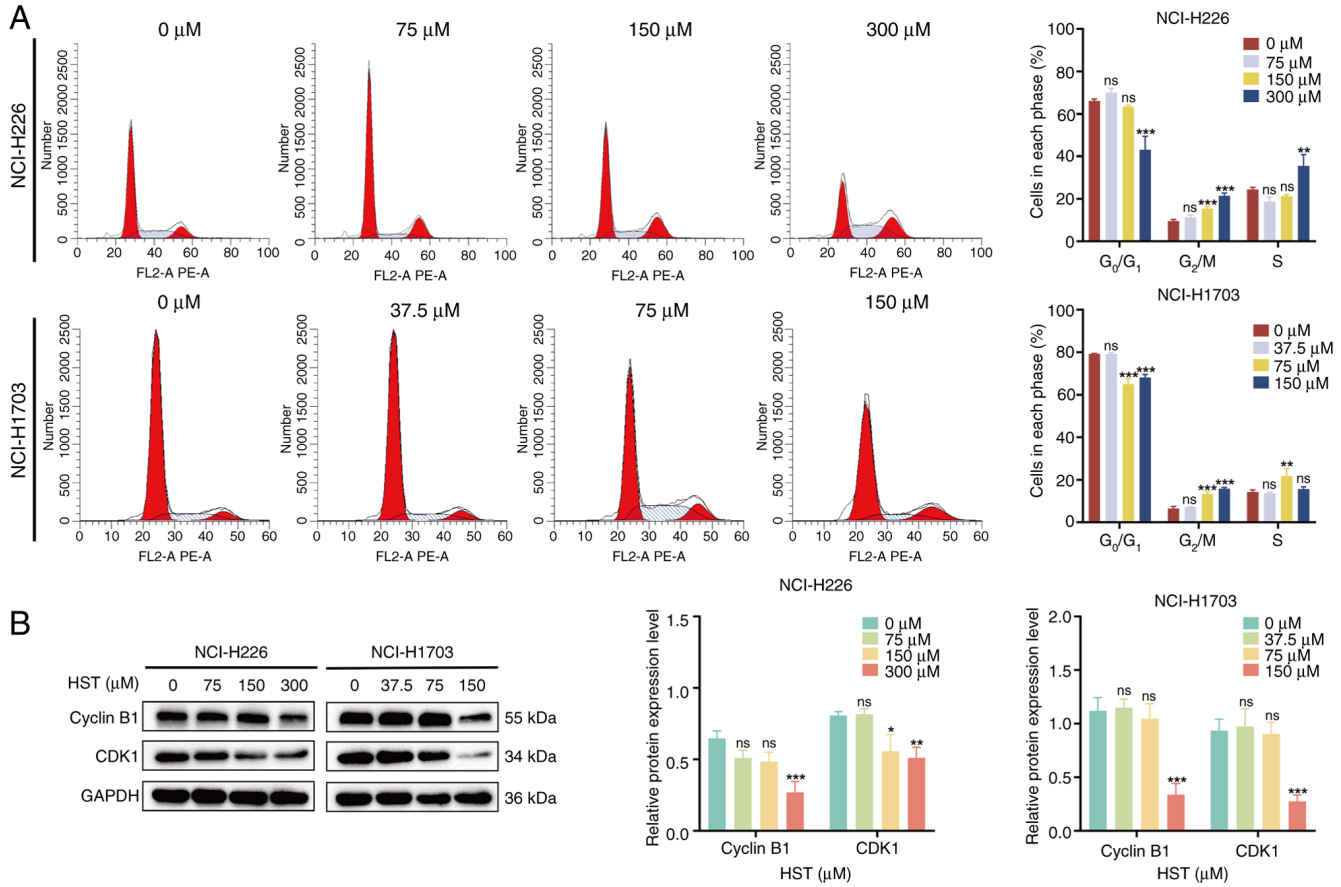

Figure 2. HST induces G_2/M phase arrest in lung squamous cell carcinoma cells. (A) Flow cytometry was used to assess the cell cycle distribution of H226 and H1703 cells after 48 h of treatment with various concentrations of HST. (B) Western blotting was used to evaluate the expression levels of cell cycle-related proteins cyclin B1 and CDK1 in H226 and H1703 cells after 48 h of treatment with different concentrations of HST. ^{ns}P>0.05, *P<0.05, **P<0.01, ***P<0.001 vs. control group. HST, hesperetin.

fluorescence ratio reflects mitochondrial membrane potential, with a decreased ratio indicating membrane potential loss, which is often associated with apoptosis. Using flow cytometry, the present study analyzed the mitochondrial membrane potential levels in HST-treated H226 and H1703 cells. The polymer/monomer fluorescence ratio of H226 cells treated with HST significantly decreased from 88.10±6.86 to 4.73±0.16% in response to HST (Fig. 3B). In H1703 cells, a statistically significant decrease in mitochondrial membrane potential was observed in the HST groups compared with that in the control group, with a decline from 87.86±7.13 to 3.31±0.44%. The degree of reduction of mitochondrial membrane potential

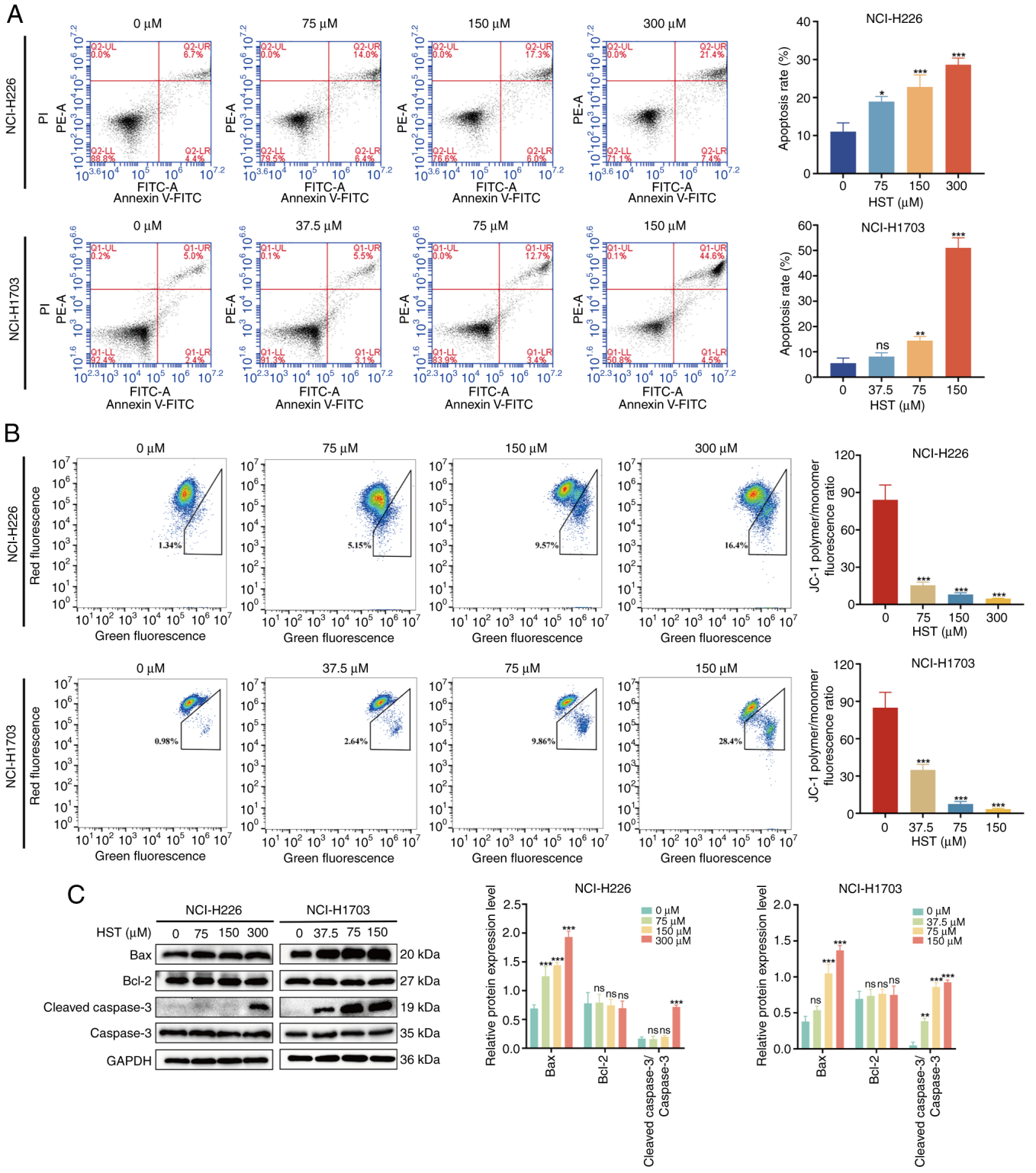

Figure 3. HST induces apoptosis in lung squamous cell carcinoma cells. (A) Annexin V-FITC/PI staining combined with flow cytometry was used to determine the apoptosis rates of H226 and H1703 cells after 48 h of intervention with different HST concentrations. (B) JC-1 staining and flow cytometry determined the mitochondrial membrane potential levels of H226 and H1703 cells after 48 h of intervention with different HST concentrations. (C) Western blotting was used to measure the expression levels of the apoptosis-related proteins Bax, Bcl-2, caspase-3 and cleaved caspase-3 in H226 and H1703 cells after 48 h of intervention with HST at given concentrations. $^{ns}P>0.05$, $^{*}P<0.05$, $^{**}P<0.01$, $^{***}P<0.001$ vs. control group. HST, hesperetin.

of H226 and H1703 cells increased with a gradual increase in HST concentration. These findings indicated that the apoptosis rate of H226 and H1703 cells gradually increased, whereas the mitochondrial membrane potential decreased with increasing HST concentrations.

Compared with in the control group, the protein expression levels of Bax and cleaved caspase-3/caspase-3 ratio in H226 and H1703 cells gradually increased in response to increasing HST concentrations (Fig. 3C). However, there was no significant decrease in the protein expression levels of

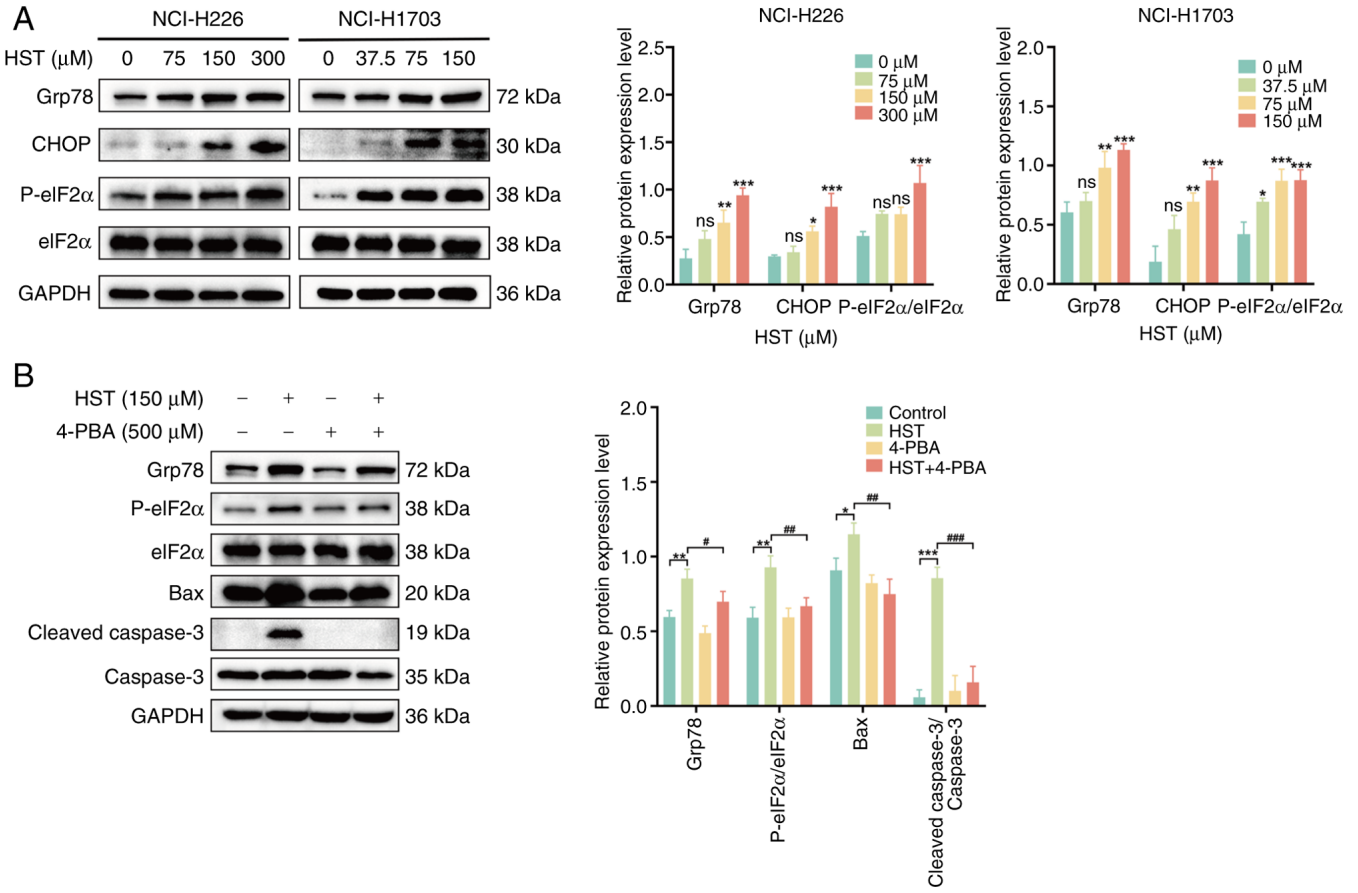

Figure 4. HST induces the apoptosis of lung squamous cell carcinoma cells by activating the endoplasmic reticulum stress pathway. (A) Western blotting detected the expression levels of endoplasmic reticulum stress-related proteins Grp78, P-eIF2α, eIF2α and CHOP in H226 and H1703 cells treated with different concentrations of HST for 48 h. (B) H1703 cells were pretreated with 500 μM 4-PBA for 6 h and were treated with 150 μM HST for 48 h. The protein expression levels of Grp78, P-eIF2α, eIF2α, Bax, caspase-3 and cleaved caspase-3 were detected by western blotting. ^{ns}P>0.05, *P<0.05, **P<0.01, ***P<0.001 vs. control group; $^{\#}$P<0.05, $^{\#\#}$P<0.01, $^{\#\#\#}$P<0.001 vs. 150 μM HST group. 4-PBA, 4-phenylbutyric acid; Grp78, glucose-regulated protein 78; HST, hesperetin; P-, phosphorylated.

Bcl-2, thus suggesting that HST may induce the apoptosis of H226 and H1703 cells by reducing mitochondrial membrane potential and increasing the expression of proapoptotic proteins.

HST induces apoptosis in LUSC cells by activating ERS. To determine whether HST induced ERS in H226 and H1703 cells, western blotting was performed to detect the protein expression levels of Grp78, P-eIF2α, eIF2α and CHOP proteins. The protein expression levels of Grp78, CHOP and P-eIF2α were progressively increased in H226 cells in response to increasing HST concentrations, with significant upregulation observed in the 300 μM group (P<0.001; Fig. 4A). Comparable trends were evident in H1703 cells, particularly in the 150 μM group, which showed a significant difference. These results suggested that HST may induce ERS in LUSC cells, and that H1703 cells have a higher sensitivity than H226 cells. Therefore, H1703 cells were selected for the subsequent functional reversibility experiments.

To determine whether HST-induced apoptosis in LUSC is associated with ERS, H1703 cells were pretreated with 4-PBA (an ERS inhibitor) for 6 h and the influence of HST on the protein expression levels of P-eIF2α, eIF2α, Grp78, Bax and cleaved caspase-3 were observed. Compared with in the 150 μM HST group, the protein expression levels of P-eIF2α, Grp78, Bax and cleaved caspase-3 were significantly reduced in the 4-PBA + HST group (Fig. 4B). These findings suggested that suppression of ERS may alleviate HST-induced apoptosis in H703 cells, and that HST could trigger apoptosis in LUSC cells by activating the ERS signaling pathway.

HST induces apoptosis in LUSC cells by inhibiting the Notch1 pathway. The Notch1 signaling pathway is also associated with apoptosis (12). Western blotting detected Notch1 and Hes-1 protein expression levels in H226 and H1703 cells. With increasing HST concentration, the protein expression levels of Notch1 and Hes-1 gradually decreased in H226 and H1703 cells, particularly in H226 cells treated with 300 μM HST and in H1703 cells treated with 150 μM HST (Fig. 5A). These findings indicated that HST inhibited the Notch1 signaling pathway in H226 and H1703 cells. H1703 cells were more sensitive than H226 cells and were selected for the subsequent functional reversibility experiments.

To confirm whether HST-induced apoptosis in LUSC cells was associated with the inhibition of Notch1 signaling, H1703 cells were pretreated with the Notch1 receptor activator Jagged-1 for 8 h. A significant increase in Notch1 and Hes-1

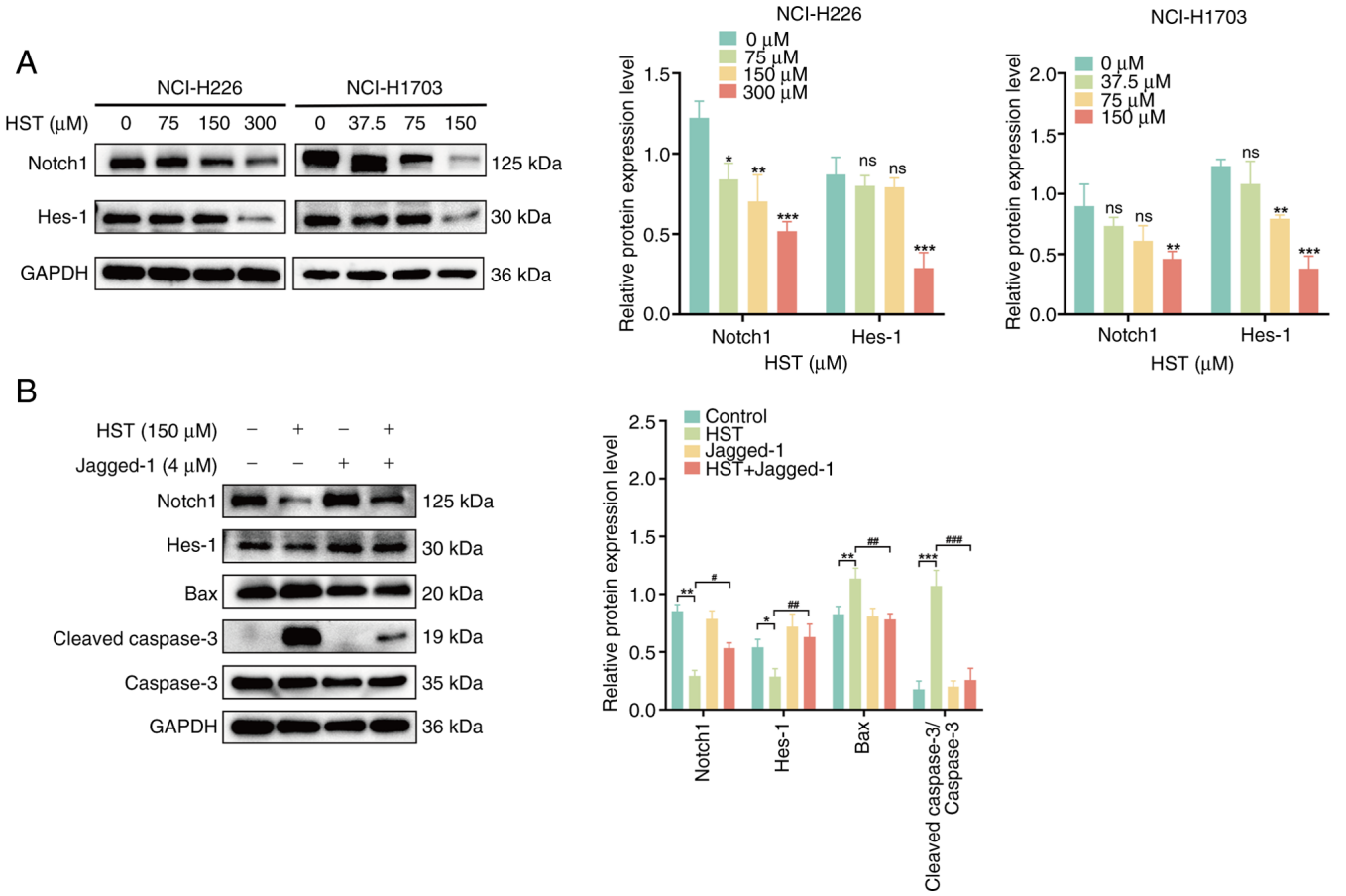

Figure 5. HST induces the apoptosis of lung squamous cell carcinoma cells by inhibiting the Notch1 signaling pathway. (A) Western blotting was used to detect the expression levels of the Notch1 signaling pathway proteins Notch1 and Hes-1 in H226 and H1703 cells treated with different concentrations of HST for 48 h. (B) H1703 cells were pretreated with 4 μM Jagged-1 for 8 h, then treated with 150 μM HST for 48 h. The protein expression levels of Notch1, Hes-1, Bax, caspase-3 and cleaved caspase-3 were detected by western blotting. ^{ns}P>0.05, *P<0.05, **P<0.01, ***P<0.001 vs. control group; $^{\#}$P<0.05, $^{\#\#}$P<0.01, $^{\#\#\#}$P<0.001 vs. 150 μM HST group. HST, hesperetin.

protein expression levels, and a significant decrease in Bax and cleaved caspase-3 protein expression levels was observed in the Jagged-1-pretreated group compared with those in the 150-μM HST group (P<0.05; Fig. 5B). These findings suggested that HST may promote the apoptosis of LUSC cells by inhibiting the Notch1 signaling pathway.

HST enhances ERS in LUSC cells through the Notch1 signaling pathway. Previous results have suggested that HST induces the apoptosis of LUSC cells by inhibiting the Notch1 signaling pathway and activating ERS. To investigate the association between HST-induced inhibition of Notch1 signaling and ERS activation, H1703 cells were pretreated with 4-PBA and Jagged-1. There was no significant change in the protein expression levels of Notch1 and Hes-1 in the 4-PBA pretreatment group compared with those in the HST group (Fig. 6A). However, the Jagged-1 pretreatment group exhibited a significant decrease in P-eIF2α and Grp78 protein expression levels and P-eIF2α/eIF2α ratio compared with those in the HST group (Fig. 6B), thus implying that the inhibition of Notch1 signaling may lead to ERS.

Effect of HST on lung squamous cells xenograft tumors in vivo. The present study evaluated the anticancer effects of HST *in vivo* using a xenograft tumor model of H1703 cells in BALB/c male

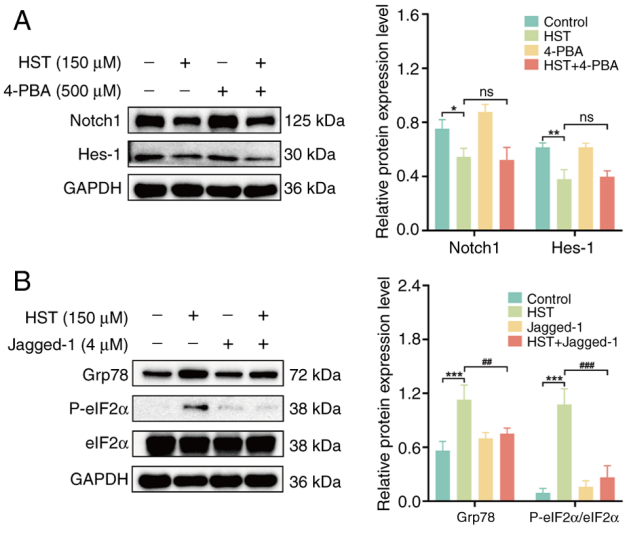

Figure 6. HST induces the apoptosis of lung squamous cell carcinoma cells by activating endoplasmic reticulum stress via the Notch1 signaling pathway. (A) H1703 cells were pretreated with 500 μM 4-PBA for 6 h, then treated with 150 μM HST for 48 h. The protein expression levels of Notch1 and Hes-1 were detected by western blotting. (B) H1703 cells were pretreated with 4 μM Jagged-1 for 8 h, then treated with 150 μM HST for 48 h. The protein expression levels of Grp78, P-eIF2α and eIF2α were detected by western blotting. ^{ns}P>0.05, *P<0.05, **P<0.01, ***P<0.001 vs. control group; $^{\#\#}$P<0.01, $^{\#\#\#}$P<0.001 vs. 150 μM HST group. 4-PBA, 4-phenylbutyric acid; Grp78, glucose-regulated protein 78; HST, hesperetin; P-, phosphorylated.

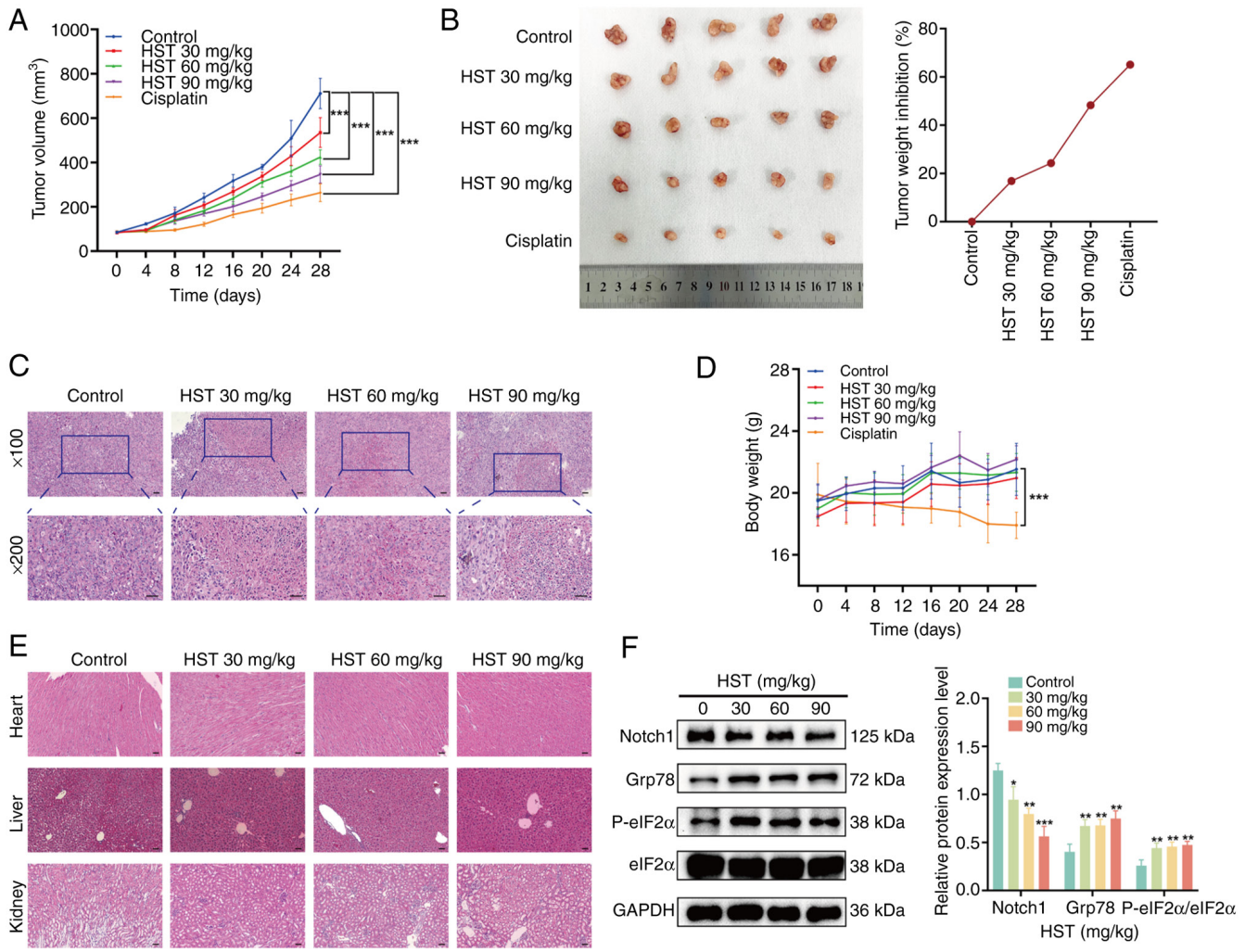

Figure 7. HST inhibits the growth of H226 nude mouse transplanted tumors *in vivo*. (A) Volume of transplanted tumors in nude mice. (B) Weight of the transplanted tumors in nude mice was recorded, and the inhibition rate of tumor weight was calculated. (C) Morphological characteristics of transplanted tumor tissues in nude mice were documented. Scale bar, 300 μm. (D) Body weight of nude mice was determined. (E) Histopathological features of key organs (heart, liver and kidney) were determined. Scale bar, 300 μm. (F) Western blotting was used to detect the expression levels of Notch1, Grp78, eIF2α and P-eIF2α in transplanted tumor tissues of the nude mice. *P<0.05, **P<0.01, ***P<0.001 vs. control group. Grp78, glucose-regulated protein 78; HST, hesperetin; P-, phosphorylated.

nude mice. No nude mice died during the treatment. Compared with in the control group, both cisplatin and HST significantly inhibited tumor growth (Fig. 7A). A dose of 90 mg/kg HST inhibited tumor growth, with an inhibition rate of 48.22% (Fig. 7B). Histopathological analysis showed that HST had a specific suppressive effect on transplanted tumors in nude mice. With increasing HST concentration, necrotic areas expanded, cell spacing widened, and cellular and nuclear debris were irregularly distributed (Fig. 7C). Notably, the body weights of mice treated with HST showed no significant changes compared with those in the control group; however, noticeable weight loss was observed in the cisplatin group during treatment (Fig. 7D). Furthermore, no drug-induced lesions were observed in the vital organs of the mice treated with 90 mg/kg HST (Fig. 7E).

The current measured the expression levels of Notch1, Grp78, P-eIF2α and eIF2α in tumors using western blot analysis. In the HST-treated groups, the levels of Grp78 and P-eIF2α were significantly increased, whereas the levels of Notch1 were gradually decreased compared with those in the control group (Fig. 7F). These findings indicated that HST may suppress tumor growth by triggering ERS and reducing the activity of the Notch1 pathway.

Discussion

HST is a natural flavonoid found in citrus fruits, grapefruit and other fruits (13), which has pharmacological effects, including anti-inflammatory, antioxidant, antiviral and antitumor properties. The present study revealed that HST can effectively inhibit the proliferation of H1703 and H226 cells *in vitro* and *in vivo*, as demonstrated by G_2/M cell cycle arrest, apoptosis induction, Notch1 signaling suppression and activation of ERS.

Cell cycle regulation is closely associated with cell proliferation, and precise control of cancer cell proliferation is crucial for cancer prevention and treatment (14). The prolonged blockade of tumor cells in the G_2/M phase serves a dual purpose: It inhibits tumor growth, while simultaneously inducing the accumulation of DNA damage and subsequent apoptosis. Consequently, targeting the G_2/M phase has emerged as a promising strategy for cancer therapy (15).

Cyclin B and CDK1 are essential regulators of the G_2/M phase transition in the cell cycle. Cyclin B is synthesized at the end of G_1 phase, peaks at the end of G_2 phase and during M phase, and forms the cyclin B-CDK1 complex in the nucleus, thereby promoting the transition from G_2 phase to mitosis. Notably, DNA damage can reduce the expression of CDK1 and cyclin B1, indicating cell cycle arrest at the G_2/M phase (16). The present study showed that HST dose-dependently arrested H1703 and H226 cells in the G_2/M phase. In addition, HST significantly reduced the protein levels of cyclin B1 and CDK1. The effect of HST on the expression of cell cycle-related proteins was consistent with cellular blockade at G_2/M phase. Therefore, the inhibitory effect of HST on the proliferation of H226 and H1703 cells may be due to the induction of cellular blockade in the G_2/M phase.

Apoptosis can be divided into the endogenous mitochondrial pathway, endogenous ERS pathway and exogenous death receptor pathway (17). Notably, mitochondria serve a crucial role in the regulation of apoptosis. Upon receiving apoptotic signals, the proapoptotic protein Bax, initially located in the cytoplasm, migrates to the mitochondrial surface, forming a pore penetrating the mitochondrial membrane. This action reduces the membrane potential and increases membrane permeability, leading to the release of apoptotic factors. The key regulatory genes involved in apoptosis, namely Bcl-2 and Bax, control the downstream activation of caspase-3 proteases and facilitate apoptotic cell death. A higher Bcl-2/Bax ratio indicates an increased resistance to apoptosis (18). The present study showed that HST reduced the mitochondrial membrane potential in a concentration-dependent manner, increased the rate of apoptosis, and upregulated the protein expression levels of cleaved caspase-3 while simultaneously decreasing the Bcl-2/Bax ratio in H226 and H1703 cells. Caspase-3, a death execution protease, is a common downstream effector in several apoptotic signaling pathways.

It has previously been suggested that ERS is crucial in tumor progression, metastasis, tumorigenesis and cell survival (19). ERS not only initiates cell survival mechanisms but also induces apoptosis. When an ERS signal is present, PKR-like ER kinase dissociates from Grp78 and activates CHOP gene transcription via the PERK/eIF2α signaling pathway, facilitating the expression of the anti-apoptotic gene Bcl-2 and cell apoptosis (20). The current study showed that HST upregulated the expression levels of Grp78, P-eIF2α, CHOP and cleaved caspase-3, which was significantly attenuated by 4-PBA (an ERS inhibitor). These results suggested that HST may induce apoptosis in LUSC cells via the ERS pathway. Previous studies have shown that certain flavonoids, including luteolin, licochalcone A and wogonoside, promote ERS-induced apoptosis in lung cancer cells (21-23).

It has also been shown that abnormal activation of Notch signaling is important in cancer progression through the maintenance of cancer stem cells (24). The functions of the Notch1 signaling pathway vary among different NSCLC subtypes (25,26). The expression of Notch1 protein in LUSC has been reported to be significantly higher than that in normal lung tissue (27), and the Notch1 expression level is positively associated with disease progression, metastasis and poor survival rates in patients (28,29). Inhibition of Notch1 signaling can induce apoptosis in LUSC cells in both a caspase-dependent and non-caspase-dependent manner (30). Some flavonoids, such as dihydromyricetin, rutin and xanthohumol, trigger apoptosis by inhibiting the Notch1 pathway in cancer cells (31-33). The present study revealed that HST inhibited the Notch1 signaling pathway in H226 and H1703 cells in a concentration-dependent manner. Furthermore, Jagged-1 (a Notch1 receptor activator) weakened the inhibitory effects of HST on the Notch1 signaling pathway and reduced HST-induced upregulation of cleaved caspase-3 expression, suggesting that HST may induce the apoptosis of LUSC cells and inhibit the Notch1 signaling pathway.

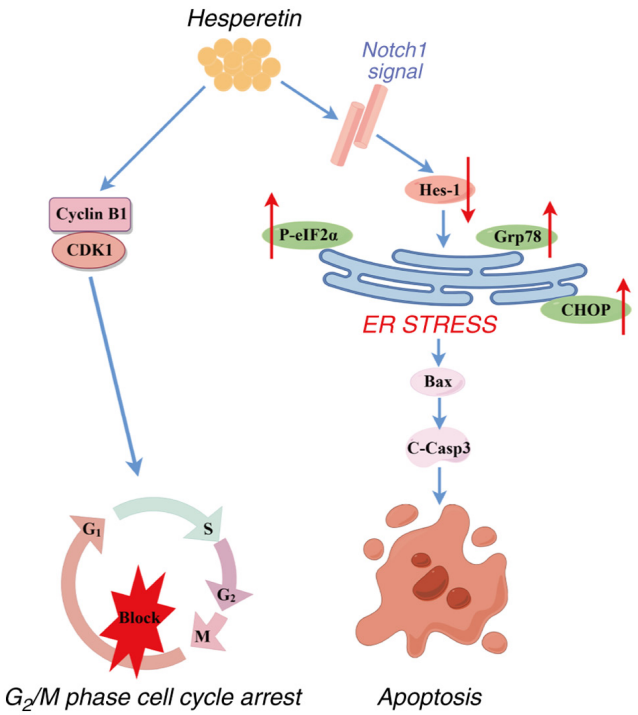

Figure 8. Mechanism and signaling pathways of the inhibitory effects of HST on the proliferation of LUSC cells. HST inhibited the proliferation of LUSC cells by inducing G_2/M phase arrest, suppressing the Notch1 signaling pathway to induce ER stress, and ultimately leading to apoptosis of LUSC cells. This figure was drawn using Figdraw (https://www.figdraw.com/). C-Casp3, cleaved capase-3; ER, endoplasmic reticulum; Grp78, glucose-regulated protein 78; HST, hesperetin; LUSC, lung squamous cell carcinoma.

Studies have shown that ERS activates the Notch1 signaling pathway (34), whereas activation of the Notch1 signaling pathway can inhibit the occurrence of ERS (35,36). Furthermore, Notch1 inhibition may enhance ERS-induced apoptosis in chronic lymphocytic leukemia cells, suggesting the involvement of the Notch1 pathway in the modulation of adaptive or apoptotic responses to ERS (37). The present results showed that Jagged-1 reduced the HST-induced upregulation of ERS-related protein expression levels in H1703 cells, whereas 4-PBA did not alter the inhibitory effects of HST on the Notch1 signaling pathway, indicating that HST may promote apoptosis in H1703 cells by activating ERS via inhibition of the Notch1 signaling pathway. Western blot analysis of transplanted tumors confirmed that HST inhibited the expression of Notch1, and increased the expression of Grp78 and P-eIF2α, consistent with the *in vitro* experimental results.

The present study identified a link between Notch1 and ERS in the apoptosis of LUSC cells but did not clarify how

Notch1 regulates ERS. Barcelos *et al* (38) revealed that the downregulation of the Notch1 pathway may activate ERS and trigger cell death by inhibiting the expression of Nrf2. Bodduluru *et al* (39) showed that HST reduces the expression of Nrf2 in lung cancer cells; therefore, Nrf2 may be a target of Notch1 and ERS.

In conclusion, the present study showed that HST inhibited the proliferation of LUSC cells *in vivo* and *in vitro*, and confirmed the association between the Notch1 and ERS signaling pathways in LUSC cells (Fig. 8). These findings may expand the understanding of how HST promotes the apoptosis of lung cancer cells and provide new ideas for treating lung cancer. These results demonstrated the potential of HST as a promising therapeutic agent for LUSC.

Acknowledgements

Not applicable.

Funding

The present study was supported by Fujian Provincial Health Technology Project (grant no. 2021CXA002), as well as grants from the High-level Hospital Foster Grants from Fujian Provincial Hospital of China (grant no. 2019HSJJ25) and the Fujian Provincial Natural Science Foundation Project of China (grant nos. 2022J01406 and 2022J011013).

Availability of data and materials

The data generated in the present study may be requested from the corresponding author.

Authors' contributions

QX was responsible for conducting the experiments, analyzing data, generating figures and table, and writing the manuscript. ZH and LT were responsible for generating figures and table and designing the methodology. ML and MZ were responsible for designing the methodology. CL was responsible for generating figures and table, and analyzing data. SC was responsible for conceptualization. LJ was responsible for conceptualization, funding acquisition, and writing, reviewing and editing the manuscript. YS was responsible for conceptualization, supervising the experiments, funding acquisition, and writing, reviewing and editing the manuscript. QX and YS confirm the authenticity of all the raw data. All authors read and approved the final version of the manuscript.

Ethics approval and consent to participate

The animal study was reviewed and approved by the Experimental Animal Welfare Ethics Committee of Fujian Provincial Hospital [approval no. IACUC-FPH-PZ-20240424(0006)].

Patient consent for publication

Not applicable.

Competing interests

The authors declare that they have no competing interests.

References

1. Li C, Lei S, Ding L, Xu Y, Wu X, Wang H, Zhang Z, Gao T, Zhang Y and Li L: Global burden and trends of lung cancer incidence and mortality. Chin Med J (Engl) 136: 1583-1590, 2023.
2. Oncology Society of Chinese Medical Association; Chinese Medical Association Publishing House: Chinese Medical Association guideline for clinical diagnosis and treatment of lung cancer (2023 edition). Zhonghua Yi Xue Za Zhi 103: 2037-2074, 2023 (In Chinese).
3. Wang J, Shen Q, Shi Q, Yu B, Wang X, Cheng K, Lu G and Zhou X: Detection of ALK protein expression in lung squamous cell carcinomas by immunohistochemistry. J Exp Clin Cancer Res 33: 109, 2014.
4. Arora S, Sheoran S, Baniya B, Subbarao N, Singh H, Prabhu D, Kumar N, Pawar SC and Vuree S: Hesperidin's role in the treatment of lung cancer: In-silico and In-vitro findings. In Silico Pharmacol 12: 104, 2024.
5. Drilon A, Rekhtman N, Ladanyi M and Paik P: Squamous-cell carcinomas of the lung: Emerging biology, controversies, and the promise of targeted therapy. Lancet Oncol 13: e418-e426, 2012.
6. Sohel M, Sultana H, Sultana T, Al Amin M, Aktar S, Ali MC, Rahim ZB, Hossain MA, Al Mamun A, Amin MN and Dash R: Chemotherapeutic potential of hesperetin for cancer treatment, with mechanistic insights: A comprehensive review. Heliyon 8: e08815, 2022.
7. Li L, Ren Z, Zhao P and Liu X: Research progress in antitumor pharmacological activities of hesperidin and hesperetin. Acta Chin Med 33: 2304-2308, 2018 (In Chinese).
8. Elango R, Athinarayanan J, Subbarayan VP, Lei DKY and Alshatwi AA: Hesperetin induces an apoptosis-triggered extrinsic pathway and a p53-independent pathway in human lung cancer H522 cells. J Asian Nat Prod Res 20: 559-569, 2018.
9. Wolfram J, Scott B, Boom K, Shen J, Borsoi C, Suri K, Grande R, Fresta M, Celia C, Zhao Y, *et al*: Hesperetin liposomes for cancer therapy. Curr Drug Deliv 13: 711-719, 2016.
10. Ramteke P and Umesh CSY: Hesperetin, a Citrus bioflavonoid, prevents IL-1β-induced inflammation and cell proliferation in lung epithelial A549 cells. Indian J Exp Biol 57: 7-14, 2019.
11. Chaudhari A, Seol JW, Kim SJ, Lee YJ, Kang HS, Kim IS, Kim NS and Park SY: Reactive oxygen species regulate Bax translocation and mitochondrial transmembrane potential, a possible mechanism for enhanced TRAIL-induced apoptosis by CCCP. Oncol Rep 18: 71-76, 2007.
12. Shi Q, Xue C, Zeng Y, Yuan X, Chu Q, Jiang S, Wang J, Zhang Y, Zhu D and Li L: Notch signaling pathway in cancer: From mechanistic insights to targeted therapies. Signal Transduct Target Ther 9: 128, 2024.
13. Babukumar S, Vinothkumar V and Ramachandhiran D: Modulating effect of hesperetin on the molecular expression pattern of apoptotic and cell proliferative markers in 7,12-dimethylbenz(a)anthracene-induced oral carcinogenesis. Arch Physiol Biochem 126: 430-439, 2020.
14. Canaud G and Bonventre JV: Cell cycle arrest and the evolution of chronic kidney disease from acute kidney injury. Nephrol Dial Transplant 30: 575-583, 2015.
15. Jiang L, Liu Y, Tumbath S, Boudreau MW, Chatkewitz LE, Wang J, Su X, Zahid KR, Li K, Chen Y, *et al*: Isopentyl-deoxynboquinone induces mitochondrial dysfunction and G2/M phase cell cycle arrest to selectively kill NQO1-positive pancreatic cancer cells. Antioxid Redox Signal 41: 74-92, 2024.
16. Zou X, Qu Z, Gao P, Sun S and Ji Y: Effects of Sulforaphane on G2/M phase arrest in HepG-2 cells and the expression of Cdk1 and CyclinB1. Acta Chin Med Pharmacol 38: 8-12, 2010 (In Chinese).
17. Krueger A, Baumann S, Krammer PH and Kirchhoff S: FLICE-inhibitory proteins: Regulators of death receptor-mediated apoptosis. Mol Cell Biol 21: 8247-8254, 2001.
18. Walensky LD: BCL-2 in the crosshairs: Tipping the balance of life and death. Cell Death Differ 13: 1339-1350, 2006.
19. Kato H and Nishitoh H: Stress responses from the endoplasmic reticulum in cancer. Front Oncol 5: 93, 2015.
20. Faitova J, Krekac D, Hrstka R and Vojtesek B: Endoplasmic reticulum stress and apoptosis. Cell Mol Biol Lett 11: 488-505, 2006.

21. Park SH, Park HS, Lee JH, Chi GY, Kim GY, Moon SK, Chang YC, Hyun JW, Kim WJ and Choi YH: Induction of endoplasmic reticulum stress-mediated apoptosis and non-canonical autophagy by luteolin in NCI-H460 lung carcinoma cells. Food Chem Toxicol 56: 100-109, 2013.
22. Qiu C, Zhang T, Zhang W, Zhou L, Yu B, Wang W, Yang Z, Liu Z, Zou P and Liang G: Licochalcone a inhibits the proliferation of human lung cancer cell lines A549 and H460 by inducing G2/M cell cycle arrest and ER stress. Int J Mol Sci 18: 1761, 2017.
23. Chen S, Wu Z, Ke Y, Shu P, Chen C, Lin R and Shi Q: Wogonoside inhibits tumor growth and metastasis in endometrial cancer via ER stress-Hippo signaling axis. Acta Biochim Biophys Sin (Shanghai) 51: 1096-1105, 2019.
24. Saran U, Chandrasekaran B, Tyagi A, Shukla V, Singh A, Sharma AK and Damodaran C: Corrigendum: A small molecule inhibitor of Notch1 modulates stemness and suppresses breast cancer cell growth. Front Pharmacol 14: 1207589, 2023.
25. Sun J, Dong M, Xiang X, Zhang S and Wen D: Notch signaling and targeted therapy in non-small cell lung cancer. Cancer Lett 585: 216647, 2024.
26. Anusewicz D, Orzechowska M and Bednarek AK: Lung squamous cell carcinoma and lung adenocarcinoma differential gene expression regulation through pathways of Notch, Hedgehog, Wnt, and ErbB signalling. Sci Rep 10: 21128, 2020.
27. Zong D, Ouyang R, Li J, Chen Y and Chen P: Notch signaling in lung diseases: Focus on Notch1 and Notch3. Ther Adv Respir Dis 10: 468-484, 2016.
28. Zhou L, Wu S, Yu L, Gong X, Song W and Cheng Z: Expression of CD133 and Notch1 in non-small cell lung cancer and the clinicopathological significance. Nan Fang Yi Ke Da Xue Xue Bao 35: 196-201 (In Chinese).
29. Yuan X, Wu H, Xu H, Han N, Chu Q, Yu S, Chen Y and Wu K: Meta-analysis reveals the correlation of Notch signaling with non-small cell lung cancer progression and prognosis. Sci Rep 5: 10338, 2015.
30. Cao H, Hu Y, Wang P, Zhou J, Deng Z and Wen J: Down-regulation of Notch receptor signaling pathway induces caspase-dependent and caspase-independent apoptosis in lung squamous cell carcinoma cells. APMIS 120: 441-450, 2012.
31. Lu CJ, He YF, Yuan WZ, Xiang LJ, Zhang J, Liang YR, Duan J, He YH and Li MY: Dihydromyricetin-mediated inhibition of the Notch1 pathway induces apoptosis in QGY7701 and HepG2 hepatoma cells. World J Gastroenterol 23: 6242-6251, 2017.
32. Khan F, Pandey P, Jha NK, Khalid M and Ojha S: Rutin mediated apoptotic cell death in caski cervical cancer cells via Notch-1 and Hes-1 downregulation. Life (Basel) 11: 761, 2021.
33. Kunnimalaiyaan S, Sokolowski KM, Balamurugan M, Gamblin TC and Kunnimalaiyaan M: Xanthohumol inhibits Notch signaling and induces apoptosis in hepatocellular carcinoma. PLoS One 10: e0127464, 2015.
34. Tremblay I, Paré E, Arsenault D, Douziech M and Boucher MJ: The MEK/ERK pathway promotes NOTCH signalling in pancreatic cancer cells. PLoS One 8: e85502, 2013.
35. Zhang M, Yu LM, Zhao H, Zhou XX, Yang Q, Song F, Yan L, Zhai ME, Li BY, Zhang B, *et al*: 2,3,5,4'-Tetrahydroxystilbene-2-O-β-D-glucoside protects murine hearts against ischemia/reperfusion injury by activating Notch1/Hes1 signaling and attenuating endoplasmic reticulum stress. Acta Pharmacol Sin 38: 317-330, 2017.
36. Gan L, Liu Z, Wu T, Feng F and Sun C: αMSH promotes preadipocyte proliferation by alleviating ER stress-induced leptin resistance and by activating Notch1 signal in mice. Biochim Biophys Acta Mol Basis Dis 1863: 231-238, 2017.
37. Silva Barcelos EC, Rompietti C, Adamo FM, Dorillo E, De Falco F, Del Papa B, Baldoni S, Nogarotto M, Esposito A, Capoccia S, *et al*: NOTCH1-mutated chronic lymphocytic leukemia displays high endoplasmic reticulum stress response with druggable potential. Front Oncol 13: 1218989, 2023.
38. Barcelos ECS, Rompietti C, Adamo FM, Dorillo E, De Falco F, Del Papa B, Baldoni S, Nogarotto M, Esposito A, Capoccia SJ, *et al*: NOTCH1-mutated chronic lymphocytic leukemia displays high endoplasmic reticulum stress response with druggable potential. Front Oncol 13: 1218989, 2023.
39. Bodduluru LN, Kasala ER, Barua CC, Karnam KC, Dahiya V and Ellutla M: Antiproliferative and antioxidant potential of hesperetin against benzo(a)pyrene-induced lung carcinogenesis in Swiss albino mice. Chem Biol Interact 242: 345-352, 2015.